Measurement 106 (2017) 221–235

Contents lists available at ScienceDirect

Measurement

journal homepage: www.elsevier.com/locate/measurement

# Environmental monitoring network along a mountain valley using embedded controllers

Víctor Villagrán [a,*], Aldo Montecinos [a], Cristian Franco [a], Ricardo C. Muñoz [b]

[a] Departamento de Geofísica, Universidad de Concepción, Chile
[b] Departamento de Geofísica, Universidad de Chile, Chile

ARTICLE INFO

*Article history:*
Received 1 July 2016
Received in revised form 22 February 2017
Accepted 27 February 2017
Available online 10 March 2017

*Keywords:*
Embedded controllers
Microcontrollers
Sensors
Environmental monitoring
Meteorological station

ABSTRACT

This paper presents the design and implementation of an atmospheric observing system to study downslope winds in the Laja River Valley, southern-central Chile. Practical design issues are discussed based on the first two years of operation, as well as scientific results that demonstrate the potential of the measurement system. The system consists of a network of eight meteorological stations that characterize the winds along the Laja River Valley, Chile. The meteorological network extends over 90 km, beginning with the station at the Antuco Ski Center at 1395 m.a.s.l. and ending at the Charrua Electric Plant at 153 m.a.s.l. The meteorological stations were designed to employ an embedded controller and high-performance instruments with low power consumption. In order to transmit data to the base station, a communication protocol was developed using SMS messages. Graphic tools are also available in the project webpage to visualize received data. Data reported in this work show that the meteorological network is able to identify and characterize downslope winds.



## 1. Introduction

Downslope winds have been studied in mountains all over the world and they exhibit one common characteristic: in certain conditions they can become dangerous windstorms. A complete study of the downslope winds requires in-situ observations because their origin and behavior are highly sensitive, among other local factors, to the existing topography which can amplify their strength. In this work an observational system is developed to study downslope winds along the Laja River Valley – Chile, located at ~37.4°S in the west side of the Andes Mountain in South America. Downslope winds in the Laja River Valley, locally known as "*Puelche*" winds, are common all year round, affecting the communities located in the front line of the effects of this phenomenon. *Puelche* events involve warm, dry and strong winds that in extreme cases can lead to fire alert conditions. Due to the lack of meteorological stations in the study area, special care should be taken in the selection of the observing technologies to monitor the phenomena, being data quality the most important concern. Since the study area is surrounded by mountains that are snow-covered in winter, the proper use of batteries and solar panels to power meteorological stations is a concern as well. Lead-acid battery performance, for instance, can decline 20% at zero degrees Celsius [1], and solar radiation decreases dramatically in winter at these latitudes. Solar panels are not an adequate solution as they can be covered by snow for long periods, with consequent effects on their performance. Thus, the meteorological stations should be powered only by batteries. With this restriction, the meteorological stations have to be highly power-efficient. The chances of vandalism are reduced in stations without solar panels, which is a real concern in remote places.

According to the authors of [2], the Santa Ana is a downslope wind in Southern California, USA, that has similarities to the *Puelche* wind. In 2007, one of the largest fires in California history was driven by especially strong Santa Ana winds [3]. Using data provided by local automated weather stations in California, some weather prediction models have been validated [3–5] for which a high spatial resolution in the observations is required (<4-km horizontal grid spacing).

As a first approach to building the meteorological network required for this project, we took a look at commercial solutions offered by the instrumentation market. With more than three decades since the company was founded, Campbell Scientific Inc. (CSI) has provided advanced data loggers and sensors that can be configured using high-level programming language. This equipment offers a rugged solution, as well as low development time, which ultimately can reduce operating costs. CSI systems are widely used in meteorology [6,7], but also in hydrology [8], oceanography [9],

* Corresponding author at: Department of Geophysics, Faculty of Physical and Mathematical Sciences, University of Concepción, Casilla-160 C, Concepción, Chile.
*E-mail address:* victor@dgeo.udec.cl (V. Villagrán).

http://dx.doi.org/10.1016/j.measurement.2017.02.046
0263-2241/

**Nomenclature**

| | | | |
|---|---|---|---|
| GSM | global system for mobile communication | IDE | integrated development environment |
| SMS | short message service | LP3500 | embedded controller |
| SIM | subscriber identity module | WXT520 | multi-sensor |
| RTC | real time clock | M10 | GSM modem |
| SRAM | static random access memory | WINDCAP | wind module |
| EEPROM | electrically erasable programmable read-only memory | RAINCAP | rain module |
| Sx | wind speed maximum | PTU | pressure, temperature and humidity module |
| Sm | wind speed average | St | station |
| Dm | wind direction average | m.a.s.l. | meters above sea level |
| Ta | air temperature | EMN | environmental monitoring network |
| Ua | relative humidity | AWS | automated weather stations |
| Pa | atmospheric pressure | | |

limnology [10] and other fields of applied physics [11]. Meteorological measurements to study the climatic change in the Demokeya forest (Sudan), for instance, were logged with CSI's CR-1000 data logger, which sampled every 6 s, and averaged/stored every 30 min [12]. Authors of [13] described an observing network dedicated to monitoring extreme weather events in California, USA. Extratropical winter storms on the North American west coast represent risks to lives and property, requiring coordinated actions to reduce negative effects. Their observing system supports the management of water supply and emergencies in California, as well as providing inputs for a numerical weather forecasting model. The network is composed of 43 CSI meteorological stations that transmit real-time data every hour. Among the meteorological measurement systems in Chile, CEAZA-MET is a network of 35 stations clustered around Coquimbo Region (30°S, 70.3°W). CEAZA (Center for Advanced Studies of Arid Zones) has operated these stations since year 2010. The stations employ the CSI CR-1000 data logger and provide meteorological data to validate climate models that help to understand and predict events such as droughts and frosts. This network takes hourly measurements of essential parameters, including air temperature, relative humidity, atmospheric pressure, wind speed and direction, and solar radiation.

A second approach to implementing the meteorological network consists of introducing engineering design in the main components of the network: the data logger, sensors' technologies, and data telemetry. With the numerous microcontrollers available today in the market, there are multiple approaches to constructing data loggers. Microcontroller-based environmental monitoring systems described in the literature support, among other applications, solar energy potential assessments [14–17], precision agriculture [18,19] and provision of early warnings of environmental emergencies such as poor air quality [20]. Authors of [21] proposed a global network for monitoring solar radiation across an extended geographic region in Sierra Nevada, Spain. This solar prospecting system has fifteen automated meteorological stations using an ATmega 16 microcontroller from Atmel Corporation (http://www.atmel.com). Solar radiation measurements, air temperature, and relative humidity are sent to the base station once a day via the Global System for Mobile Communication (GSM) cellular infrastructure. A 64 KB EEPROM completes the hardware components required in the design. Authors of [22] described a low-cost microcontroller-based system to monitor crop temperature and water status. The microcontroller is a PIC16F88 from Microchip Technologies (http://www.microchip.com) that takes measurements at one-hour intervals. Current consumption is approximately 13 mA during active measurement periods, dropping to 0.34 mA in sleep mode. Authors of [23] described another application in agriculture using a MSP430F449 microcontroller from Texas Instruments (http://www.ti.com). They present a GSM-based wireless monitoring system for field information. The system automatically reports, in real-time, the environmental measurements including air temperature, relative humidity and wind speed, as well as information about the population of the oriental fruit fly using the cellular Short Message Service (SMS). Authors in [24] presented a development of a weather monitoring station intended for applications such as agriculture and farming. The data logger design is based on the PIC16F887 microcontroller and utilizes standard meteorological sensors along with signal conditioning circuits.

A slightly different alternative to the microcontrollers are the embedded controllers. With microcontrollers, part of the work involves designing the printed circuit board that integrates the microcontroller with other essential components such as a real-time clock (RTC) and a non-volatile memory for data storage. Embedded controllers can be found in different form factors, some of them adequate for the final application [25].

Authors of [26] presented an environmental monitoring system based on a Mini6410 embedded controller from FriendlyARM (http://www.friendlyarm.net). The Mini6410 is a single-board computer with multiple features, however, it could not be used as a power-efficient data logger since its consumption is up to 0.25 A. Authors of [27] describe the design of a real-time monitoring system to support research in hydrometeorology and hydrology in Iowa, USA. They report around 40 meteorological stations built on the power-efficient LP3500 embedded controller from Digi International. The board consumes less than 20 mA when fully operational and less than 100 μA when powered down. This embedded controller exhibits similar power performance to the highly power-efficient microcontrollers described before, but offering a form factor closer to a single-board computer.

Monitoring systems in remote locations, like the study site of this project, extensively use the cellular network for data telemetry [28–30]. Because of the continued growth of the mobile telecommunication industry, its coverage has also expanded in Chile, even in remote areas inhabited by small communities. Authors of [30] built a monitoring system that transmits meteorological data using GSM-SMS technology. Various performance tests over the transmitted data showed that the method is highly reliable. Thus, it is highly probable that sent and received SMS messages are the same. The SMS is the most common and economically affordable digital transmission service used for sending and receiving text messages [31]. SMS messages can be as long as 160 characters in text or binary format. The SMS is a mature service available since the second generation mobile communication technology and still present today.

In this work, the observational system should provide high spatial temporal resolution measurements, in order to characterize the full life cycle of the meteorological phenomenon. Design objectives imposed on the system are: (1) to supply high quality data to support the study of the atmospheric phenomenon of interest; (2) to have high sampling rate to detect rapid changes in the variables; (3) to transmit data in near real-time; and (4) to have a low power requirement. Each node in the network is composed of a custom-made data logger and high-performance sensors. Stations store data to intervals of one minute, and transmit data to the base station by using SMS messages.

The remainder of this paper is organized as follows. Section 2 reviews the main features of system components and how they are combined to satisfy design objectives. Electrical diagrams, software routines, and data output formats describe the design of the meteorological stations. The analysis of the system's performance and the study of measurements collected are covered in Section 3. Finally, in Section 4 we present the conclusions.

## 2. Material and methods

### 2.1. Location of the automated weather stations (AWS's)

The monitoring network, composed of eight AWS's extending over 90 km along the Laja River Valley, is shown in Fig. 1. The AWS's are distributed from the highest site at the valley head, near the Antuco ski center at 1395 m.a.s.l., to the lowest site at the Charrua Electric Plant at 153 m.a.s.l., 50 km to the west of the valley mouth. The local siting was performed following the installation's guide provided by the sensor's manufacturer [32]. Particularly important for the wind measurement is the selection of a site free from turbulence and obstructions caused by nearby objects. Additionally, the resulting network was set by the compromise of three logistic factors: security, accessibility, and availability of cellular network signal. Table 1 lists the location of each AWS, their altitudes and reference names. Only seven stations (St1–St7) were installed in February 2014. The eighth and last station (St8) named as Hotel station was installed between St3 and St4, in August 2014.

### 2.2. Description of sensors

To meet the goals of this study, we have selected the Vaisala WXT520 weather multi-sensor. Vaisala is a Finnish company (http://www.vaisala.com) that has decades of experience manufacturing high performance meteorological instruments which are widely used in scientific projects [33–35]. The WXT520 is a low power consumption equipment that contains six weather sensors that measure air temperature, relative humidity, atmospheric pressure, precipitation and wind speed and direction. The equipment is compact and easy to install and maintain, because it is designed to measure precipitation utilizing an innovative method based on a sensitive piezoelectric surface [36]. The wind speed and wind direction sensor is composed of three ultrasonic transducers and the remaining three sensors employ capacitive technology. The WXT520 is a six-in-one instrument that can be interfaced by the ubiquitous RS232 asynchronous serial interface. Direct laboratory measurements using the WXT520 show that the instrument consumes around 0.25 mA in stand-by mode and approximately 3.0 mA in normal mode when all sensors are being sampled.

The six sensors used by the WXT520 are functionally separated into three sensor modules named as: WINDCAP for wind speed and direction sensor, RAINCAP for precipitation, and PTU for air temperature, relative humidity and atmospheric pressure. The operation of the WXT520 depends on several control registers that can be set up by the Vaisala parameter setting software or through a serial terminal such as the hyperterminal on the Windows operating system. Three of these registers define the sampling strategies and the output formats for sensors on the three sensor modules: the aWU register for WINDCAP module, the aTU register for PTU module, and the aRU register for RAINCAP module. The fourth essential register is the aXU register which establishes the communication parameters. Table 2 describes performance characteristics of the six sensors contained in the WXT520 as well as the parameters of the control registers that configure the operation of the equipment. Description of the main parameters that define the control registers are provided in Table 3.

In this project, the WXT520 was configured in the polled operation mode, in which the data logger sends requests for measurements to a specific sensor module. The sampling time is defined as high as possible, in order to capture the rapid dynamics of the *Puelche* wind. According to the time response of the slowest sensors (PTU module) listed in Table 2, the sampling time was established as 60 s. Data are stored into the main memory of the AWS at a rate of 60 s, as well. As the response time of wind sensor is so much faster than the rest of the sensors, this sensor is sampled at 1 Hz and its measurements averaged and logged every 60 s.

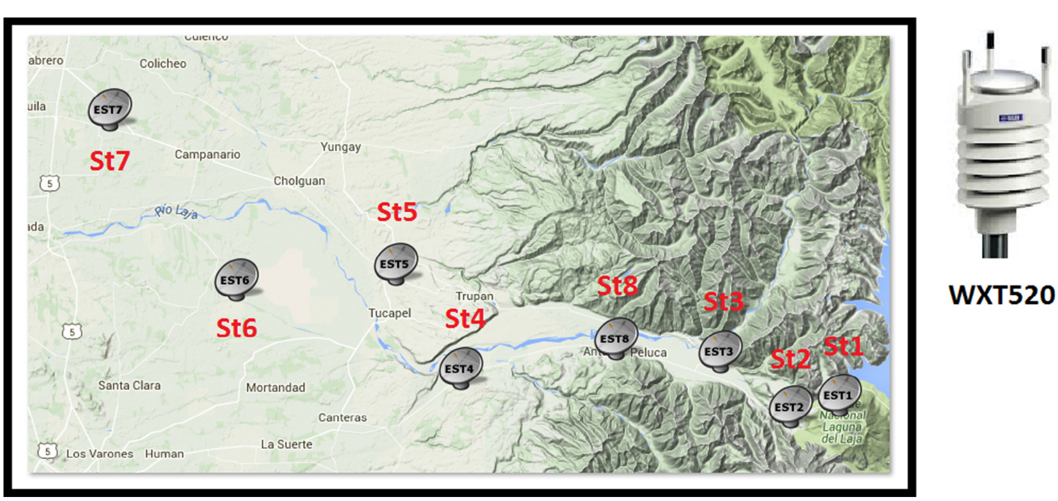


**Fig. 1.** Study area in the Laja River Valley. The WXT520 multi-sensor measures six essential meteorological parameters: air temperature, relative humidity, atmospheric pressure, wind speed, wind direction and precipitation. Station St8 was added in August 2014, while the rest of stations were installed in February 2014.

**Table 1**
Location of the automated weather stations (AWS).

| Station ID | Name | Latitude (S) | Longitude (W) | Altitude (m) | Installation date |
|---|---|---|---|---|---|
| St1 | Volcán | 37°23,141′ | 71°22,577′ | 1396 | Feb 2014 |
| St2 | Conaf | 37°32,876′ | 71°26,427′ | 958 | Feb 2014 |
| St3 | Endesa | 37°20,429′ | 71°31,857′ | 733 | Feb 2014 |
| St4 | Rucue | 37°21,480′ | 71°51,915′ | 396 | Feb 2014 |
| St5 | Carmen | 37°15,060′ | 71°56,976 | 304 | Feb 2014 |
| St6 | Lechería | 37°16,039′ | 72°9360′ | 240 | Feb 2014 |
| St7 | Charrúa | 37°5561′ | 72°19,104′ | 153 | Feb 2014 |
| St8 | Antuco | 37°19,688′ | 71°39.938′ | 560 | Aug 2014 |

**Table 2**
WXT520 performance and settings.

| | Parameter | Accuracy | Output Resolution | Time Response |
|---|---|---|---|---|
| Performance | Air temperature, Ta | ±0.3 °C at −52 to 60 °C | 0.1 °C | 20 s at 63%RH |
| | Relative humidity, Ua | ±0.3% at 0–90%RH | 0.1% RH | 12 s at 51–73% RH |
| | Atmospheric pressure, Pa | ±0.5 hPa at 0–30 °C | 0.1 hPa | <1 s |
| | Precipitation (rainfall), Rc | Better than 5% (percent of actual output reading, and it does not include possible wind induced error) | 0.01 mm | – |
| | Wind speed, Sm | ±0.3 m s$^{-1}$ or ±3% whichever is greater for the measurement range 0–35 m s$^{-1}$ | 0.1 m s$^{-1}$ | 0.25 s |
| | Wind direction, Dm | ±3° | 1° | 0.25 s |
| Settings | Module | Parameters of the register | | |
| | Communication | aXU, = 0, M = P, T = 0, C = 2, I = 0, B = 9600, D = 8, P = N, S = 1, L = 25, N = WXT520 | | |
| | PTU | aTU, R = 11010000 & 11010000, I = 60, P = H, T = C | | |
| | RAINCAP | aRU, R = 11111100 & 11111100, I = 60, U = M, S = M, M = T, Z = L, X = 65,000, Y = 1000 | | |
| | WINDCAP | aWXU, R = 11111100 & 11111100, I = 60, A = 60, G = 1, U = M, D = 0, N = W, F = 1 | | |

**Table 3**
Description of main parameters on WXT520's control registers.

| Register | Description of main parameters |
|---|---|
| aXU | A is an address number. M defines the communication protocol, in our configuration, polled mode (P). C is the type of serial interface (1 = SDI-12 or 2 = RS232). B is the baud rate |
| aTU | R defines which measurements of the PTU module are sent upon request of the data logger. R is a parameter of selection that consists of 16 bits. I is defined as the update interval. P defines the units for the atmospheric pressure. T defines the units for the temperature |
| aRU | R and I are defined as in aTU register. U is precipitation units, in our configuration, M means metric (accumulated rainfall in mm, rain duration in s, rain intensity in mm/h). M in our configuration is set as T, which means time based. The WXT520 sends a precipitation data in the intervals defined in the I parameter. Z is the counter reset, in our configuration defined as L. The rain counter or hail counter is reset, when it reaches predefined limit. X is the rain accumulation limit between 100 and 65,535, settings the rain accumulation counter resetting limit. Y is the hail accumulation limit between 100 and 65,535 |
| aWXU | R and I are defined as in aTU register. A is defined as the averaging time, or the period over which the wind speed and direction averaging is calculated. F defines how frequently the wind is measured |

### *2.3. The embedded controller*

The LP3500 from Digi international Inc. is an embedded controller designed specifically for low power applications requiring I/O control and data logging capabilities. Digi International is a communications and technology company headquartered in Minnesota, USA (https://www.digi.com). Based on the Rabbit 3000 microprocessor (https://www.digi.com/products/rabbitprocessor) from Digi international, the LP3500 incorporates 512 K of flash memory, 512 K of static RAM, digital I/O ports, A/D converter inputs, PWM outputs, and RS232/RS485 serial ports. With six serial ports, the LP3500 can easily integrate devices with serial interfaces including a modem for data transmission. The board is programmed with Dynamic C software, an integrated development environment (IDE) that provides debugging support, a library of drivers, and sample programs (https://www.digi.com/support/productdetail?pid=5053). A complete description about hardware, and software functions to program the board can be found in the user's manual [37].

The LP3500 can operate at various levels of power consumption, depending on the microprocessor clock frequency. In normal mode at the highest frequency, the microprocessor runs at a nominal speed of 7.4 MHz and when all subsystems are active, the LP3500 consumes less than 20 mA. The LP3500 consumes less than 100 μA in the power-save mode, the lowest power mode. To improve power efficiency of the LP3500, it is also possible to disable subsystems that are not being used. Particularly, the subsystems on the board are turned off using the *devPowerSet* software function, before placing the LP3500 in power-save mode.

In normal mode, the LP3500 is powered from an external battery on pin header J2. This power source is named as VIN. The LP3500 contains an on-board coin-type 3V battery that gives support to the SRAM and the RTC when power is interrupted. The on-board battery is also intended to be used in power-save mode when power is disabled. In this condition, the expected life of the on-board battery is around 240 days, which can be extended using an external secondary power source in a range of 2.8–3.3 V. The external 3 V battery referred as VBAT, is also connected on pin header J2.

#### *2.3.1. Setting the power-save mode*

Once data acquisition and other processing tasks are completed, the LP3500 waits for the next sampling cycle in an idle state. The power-efficiency of the board can significantly improve when the LP3500 is placed in power-save mode in the idle state. The LP3500 can enter into power-save mode by using the *timedAlert* software function. After calling the *timedAlert*, the board awakes when a pre-defined time has elapsed. For instance, if the sampling time is one minute and the time required to execute processing tasks is 5 s, then a pre-defined time of 55 s should be configured in the *timedAlert* function. Arguments of the *timedAlert* function define: the pre-defined time (period of time in which the processor is sleeping), the specific power mode when the board awakes and the power source used during the power-save mode, VIN or VBAT. By using the VBAT as power source during power-save mode, the internal linear voltage regulator on the board can be turned off as well, adding even more energy efficiency.

#### *2.3.2. The watchdog service*

The watchdog service is a mechanism used to detect and recover from malfunctions on the LP3500. When the watchdog service is enabled, a counter counts down from some initial value that can be configured in a range of 2–255. If the counter reaches zero, the watchdog timer will not be reset since the software got hang before. By using the *VdGetFreeWd* software function, the LP3500 creates a watchdog timer that counts down to a rate of 62.5 ms. For instance, if the *VdGetFreeWd* is configured with an initial value of 100, the LP3500 must reset the watchdog timer before 6.25 s (62.5 ms multiplied by 100); otherwise the board is reset. To reset the watchdog timer the *VdHitWd* software function must be called periodically.

### *2.4. The environmental monitoring network (EMN)*

An overall diagram of the EMN is shown in Fig. 2. Each node in the network corresponds to an automated weather station (AWS), which is composed of a WXT520 multi-sensor, a custom-made data logger, and a GSM modem. The data logger built on the LP3500 is dedicated to collect meteorological data from the WXT520 and then transmits the data to the base station at the University of Concepción, located 160 km to the west of St1. At a sampling time of one minute, data are stored into a micro SD card on the AWS. The AWS's transmit data every hour to the base station using the cellular network.

Three ASCII output files on the micro SD card save data in different formats. The first output file, called *raw* file, stores all ASCII characters coming out from WXT520 upon the data logger request in the sampling process. Output data are ASCII characters representing measurements including the name of the variables and its units. This file provides a backup of raw data received from WXT520 and it also can be useful to verify that data parsing process was correctly done. The second output file, called *meteo* file, is a high-level user-readable file that contains the measurements of the six sensors along with statistics of wind speed and direction, variables derived from precipitation such as rain duration and rain intensity, and system variables such as reference voltages. A list of variables received from the WXT520 and stored in the *meteo* file, along with time and date stamps, is shown in Table 4. The third output file, called *hexa* file, stores a copy of the hexadecimal encoded data that are transmitted to the base station. In a period of six months, around 90 MB are needed to store these three files.

#### *2.4.1. Data transmission*

The data logger stores data in intervals of one minute to provide a high resolution characterization of the *Puelche* wind. However, to reduce transmission costs, not all data are transmitted to the base station. Every hour, the AWS sends one SMS message that contains data in intervals of 15 min as described in Fig. 3. The message is constructed with header information and meteorological data. Header information includes the identification number of the AWS, the type of message, date-time stamp and system variables like battery level. A one-character parameter identifies the type of message from one of three categories: (1) data message, which is transmitted hourly; (2) start message, transmitted when the station is turned on; and (3) alert message, transmitted when the station reports an alert condition like a low battery warning or the occurrence of out-of-range measurements. Data are encoded to reduce its size, before transmission. An integer variable is directly converted into hexadecimal number, while a float variable is first converted to integer by multiplying it by a power of ten. Table 5 describes the way in which each variable is converted in a hexadecimal number to build a SMS message. The SMS message is a collection of 108 hexadecimal characters.

#### *2.4.2. Design of the automated weather station (AWS)*

The electrical diagram of the data logger is shown in Fig. 4. By using serial ports on the LP3500, the controller establishes communication with the main components of the AWS: the WXT520 multi-sensor, the micro SD card driver, and the GSM modem. The Openlog card driver from Sparkfun (https://www.sparkfun.com) creates FAT16 files, upon request of a serial command sent by

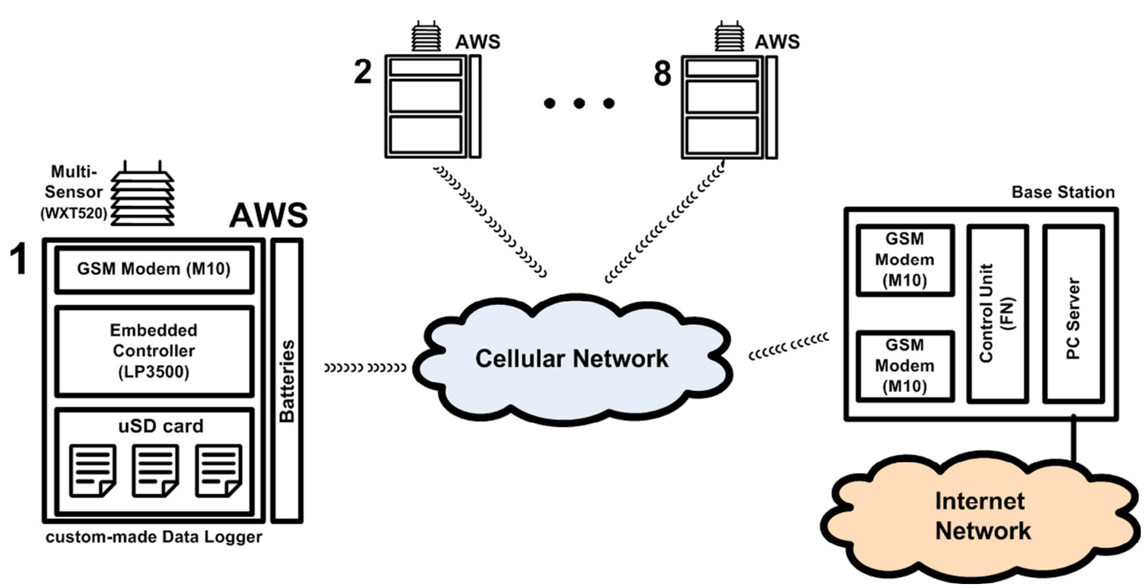


**Fig. 2.** Overall diagram of the environmental monitoring network (EMN). The network allows for characterizing downslope winds, locally known as "*Puelche* wind".

**Table 4**
Meteorological variables stored in the *meteo* file at one-minute sampling time.

| | Variable | Name | Unit (in short) | Unit |
|---|---|---|---|---|
| 1 | Wind direction minimum | Dn | D | Degree |
| 2 | Wind direction average | Dm | D | Degree |
| 3 | Wind direction maximum | Dx | D | Degree |
| 4 | Wind speed minimum | Sn | M | m/s |
| 5 | Wind speed average | Sm | M | m/s |
| 6 | Wind speed maximum | Sx | M | m/s |
| 7 | Air temperature | Ta | C | Celsius |
| 8 | Relative humidity | Ua | P | % |
| 9 | Atmospheric pressure | Pa | H | Hecto Pascal |
| 10 | Rain amount | Rc | M | Milimeter |
| 11 | Rain duration | Rd | S | Seconds |
| 12 | Rain intensity | Ri | M | mm/h |
| 13 | Hail amount | Hc | M | mm/h |
| 14 | Hail duration | Hd | S | Seconds |
| 15 | Hail intensity | Hi | M | Hits/cm$^2$ h |
| 16 | Heating temperature | Th | C | Celsius |
| 17 | Heating voltage | Vh | V | Volt |
| 18 | Supply voltage | Vs | V | Volt |
| 19 | 3.5 V reference voltage | Vr | V | Volt |

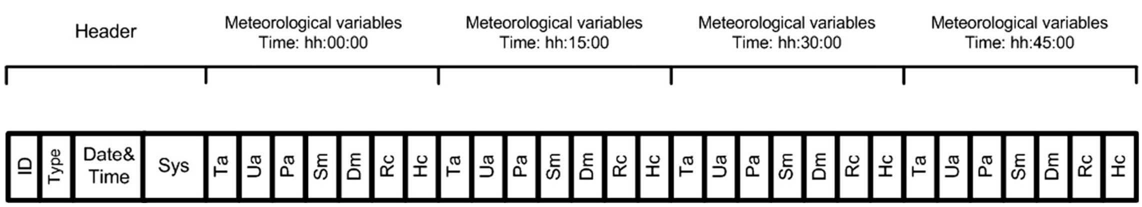


**Fig. 3.** Structure of a SMS message composed by 108 hexadecimal characters. Each message is sent every hour to the base station and it contains measurements at a rate of 15 min.

**Table 5**
Description of the output format for the SMS message sent every hour.

| Parameter | Example | Conversion factor | Encoded parameter | | Required bytes | |
|---|---|---|---|---|---|---|
| | | | Dec | Hexa | | |
| Station ID | 6 | 1 | 6 | 0x6 | 0,5 | System variables 6 bytes |
| Type of message | 0 | 1 | 0 | 0x0 | 0,5 | |
| Julian day | 30 | 1 | 30 | 0x01E | 1,5 | |
| Year | 2015 | Year-2010 | 5 | 0x5 | 0,5 | |
| Hour | 12 | 1 | 12 | 0x0B | 1,0 | |
| System battery [V] | 11.9 | 10 | 119 | 0x77 | 1,0 | |
| Heater battery [V] | 12.5 | 10 | 125 | 0x7D | 1,0 | |
| Air temperature, Ta [°C] | 20.3 | 10 | 203 | 0x2D3 | 1,5 | First meteo scan 12 bytes (12:00) |
| Relative humidity, Ua [%] | 78.1 | 10 | 781 | 0x30D | 1,5 | |
| Atmospheric pressure, Pa [HPa] | 906.3 | 10 | 9063 | 0x2367 | 2,0 | |
| Wind speed, Sm [m/s] | 6.7 | 10 | 67 | 0x043 | 1,5 | |
| Wind direction, Dm [°] | 210 | 1 | 210 | 0x0D2 | 1,5 | |
| Rain amount, Rc [mm] | 388.91 | 100 | 38,891 | 0x97 EB | 2,0 | |
| Hail amount, Hc [hits/cm$^2$] | 132.4 | 10 | 1324 | 0x0540 | 2,0 | |
| Second meteo scan (12:15) | | | – | – | 12,0 | 12 bytes |
| Third meteo scan (12:30) | | | – | – | 12,0 | 12 bytes |
| Fourth meteo scan (12:45) | | | – | – | 12,0 | 12 bytes |
| Total | | | | | 54 | 54 |
| A SMS message (108 characters) | 6001E50B777D2D330D23670430D297EB05402D330D23670430D297 EB05402D330D23670430D297EB05402D330D23670430D297EB0540 | | | | | |

the LP3500. Once the file has been created, the LP3500 sends the ASCII characters corresponding to the data. The M10 from Quectel is the GSM modem that sends the SMS messages. Quectel is company headquartered in Shanghai, China, that offers high-performance cellular technology (http://www.quectel.com). Flowcharts in Fig. 5 describe software functions that allow the LP3500 to communicate with the Openlog card driver and the GSM modem.

Each GSM modem utilizes a SIM (Subscriber Identity Module) card provided by a telecommunication company. As it is shown in Table 6, the St2 station does not have a modem since it is located in a place without cellular coverage. All the rest of AWS's have GSM modems and the SIM card provided by the telecommunication company that exhibited best cellular coverage for the corresponding site. The messages are sent using AT commands, or attention commands, to one GSM modem in the base station. AT commands

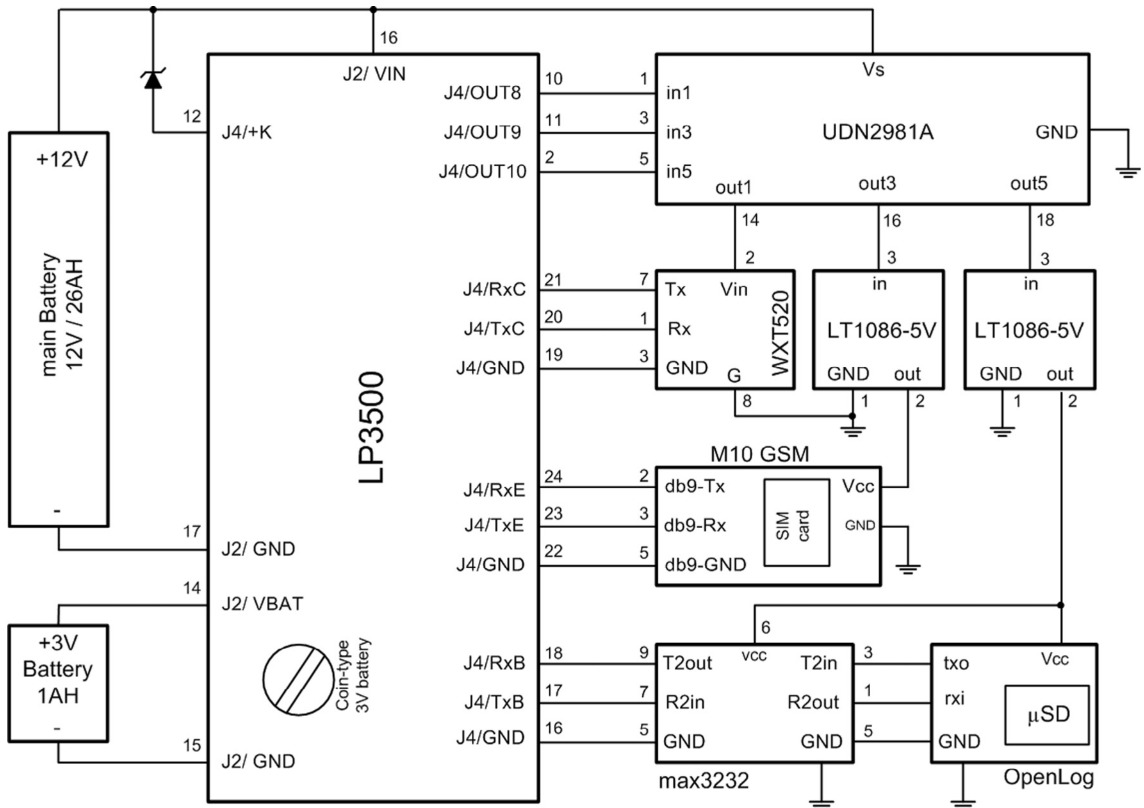


**Fig. 4.** Electrical diagram of the custom-made data logger. The meteorological stations are a hybrid between high quality commercial multi-sensor and a data logger built on an embedded controller. Data are stored at a rate of one record per minute.

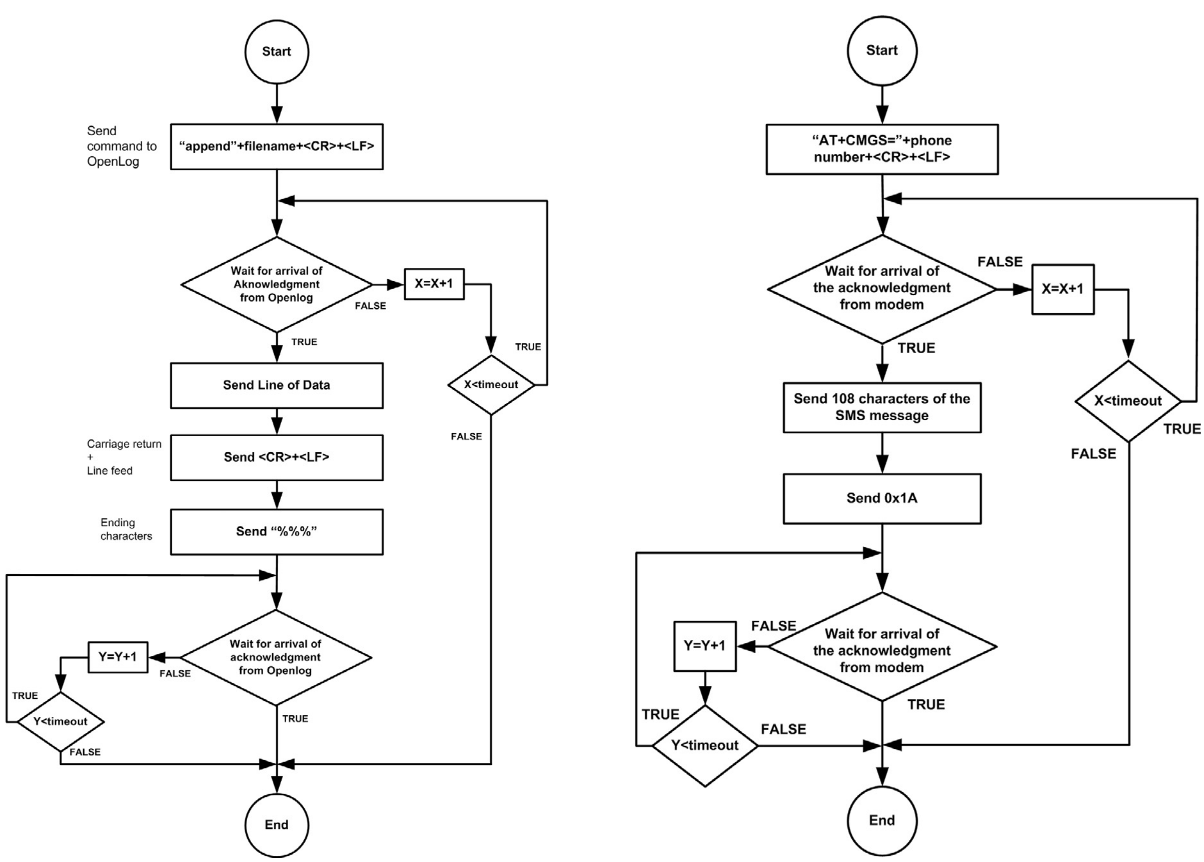


**Fig. 5.** Software flowcharts, (left) function to send a SMS message and (right) function to write on the micro SD card.

**Table 6**
Initial configuration of the automated weather stations (AWS).

| Station ID | SIM card company | Cellular coverage | Solar panels | Data logger operation mode |
|---|---|---|---|---|
| St1 | Movistar | Bad/intermittent | Not used | Power-save mode |
| St2 | – | Null | Not used | Power-save mode |
| St3 | Entel | Good | Not used | Power-save mode |
| St4 | Entel | Good | Not used | Power-save mode |
| St5 | Entel | Good | Not used | Power-save mode |
| St6 | Entel | Good | Not used | Power-save mode |
| St7 | Entel | Good | Not used | Power-save mode |
| St8 | Entel | Good | Used | Normal mode |

are a set of instructions to operate cellular devices. Table 7 describes the AT commands used in the AWS's as well as in the base station.

The main power source of the AWS is provided by a 12 V–26AH battery and two AA 1.5 V batteries in series are used as additional source to power the microprocessor when it is in power-save mode. In addition to the main power source and the external 3 V battery, a separate power source could be used to power the digital output-input circuits at terminal +K on the board. Although the use of this third power source increments the energy efficiency, a leakage less than 30 μA was obtained when +K was supplied from the +12 V battery via a zener diode. The UDN2981A is a Darlington source driver device from Allegro Microsystems (http://www.allegromicro.com) that is added to optimize power use. By using the LP3500 digital outputs, the UDN2981A is used to turn on/off external devices. Both the GSM modem and the Openlog are powered through LT1086 voltage regulators from Linear Technologies (http://www.linear.com) which are connected to output channels on USD2981A. The multi-sensor is always on, since it can manage power usage efficiently by itself. However, it is also powered through the UDN2981A, in the event the LP3500 needs reboot.

A flowchart of the main software loop in the AWS's is shown on the left side of Fig. 6. The LP3500 runs in normal mode while sampling and processing tasks are being executed. When all tasks are completed, the LP3500 is placed in power-save mode until the next sampling is required. Every minute, the LP3500 does the following: (1) it turns the Openlog on, (2) it sends data requests to WXT520, (3) it parses the received data string, (4) it appends data on *meteo* and *raw* file, and (5) it turns the Openlog off. Along the hour, some meteorological variables are extracted to build the SMS message. When the 108-character SMS message is completed, it is transmitted via the GSM modem once per hour.

In order to detect and overcome malfunctions, AWS's were also programmed using the watchdog service. The watchdog timer reboots the LP3500 unless the program explicitly restarts the watchdog by the *VdHitWd* software function. The watchdog timer is created by using the VdGetFreeeWd software function, which was configured to count 255 times at a rate of 62.5 ms. The counter takes around 15.9 s (255 multiplied by 0.0625) to reach zero. Therefore the program must send *VdHitWd*'s before 15.9 s have elapsed from the last timer restart. The watchdog service is also enabled during the power-save mode by making *timeAlert* callings shorter than 15.9 s, as it is shown on the right side of Fig. 6. Thus, the *VdHitWd's* can be done between *timeAlert* callings. The actual aspect of the custom-made data logger built on the LP3500 is shown in Fig. 7. The initial configuration of AWS's is presented in Table 6.

**Table 7**
List of AT commands to manipulate SMS messages.

| AT command | Description |
|---|---|
| "AT+CMGS="+cell number +<CR>+<LF> | Send a SMS message to the SIM card's cellular number |
| "AT+CPMS=?"+<CR>+<LF> | Ask for the number of SMS messages stored in SIM card |
| "AT+CMGR="+index+<CR> +<LF> | Read a SMS message available in SIM card's memory |
| "AT+CMGR="+index+<CR> +<LF> | Delete a SMS message from SIM card's memory |

### 2.4.3. Design of the base station

AWS's transmit meteorological variables contained in a SMS message to the base station at the University of Concepción. A web application allows the user to access the data from internet at the URL: daw.dgeo.udec.cl. It resides in an Apache web server running under GNU/Linux Debian 8. The application was implemented using PHP scripting, HTML and JavaScript languages along with libraries such as Prototype and API's (application programming Interface). The user web interface provided by the application is shown in Fig. 10. Section A presents a map of the study area showing the meteorological stations. Using a JavaScript code and the Google Maps API, a message window appears when the mouse cursor is over a station. Information about the name of the station and its altitude above sea level is deployed in the window. Section B is used to select the period of time in which the variables marked in Section are plotted. There is a graph for every selected variable, and many curves in the graph as selected stations in Section D. Interactive elements in sections B, C and D are software objects handled by programming in HTML and JavaScript, and using the Prototype library. A PostgreSQL is used as database system to administrate data received by the meteorological network. By using PHP scripting, data are inserted into a PostgreSQL database. After user request, data are accessed from the database to generate plots of predefined variables using JavaScripts and the Google Charts API.

The electrical diagram in Fig. 8 shows the hardware components required to implement the base station. It consists of three main parts: the controller, the collector machine and the web server machine. The controller is implemented using an embedded controller from Tern Inc. (http://tern.com). The embedded controller is a flashCore-N (http://tern.com/products-2/186-processor-boards/flashcore-n), a board designed for projects requiring mass serial communication capabilities. Two GSM modems are connected to the controller, because the cost for transmitting one SMS rises several times when the destination is a GSM modem that has a SIM card provided by a company different than the SIM Card on the sender modem. Using AT commands as described the flowchart in Fig. 9, the controller interrogates hourly both modems about the arrival of new SMS messages. The controller is also dedicated to clean data from additional information sent by the telecommunication company. After parsing, only 108 hexadecimal characters are serially transferred to the collector machine, a computer under GNU/Linux Debian 8 operative system, and connected to the local area network (LAN). This machine gets the hexadecimal characters by reading the serial buffer, and then characters are appended to a text file. As the web server machine is also

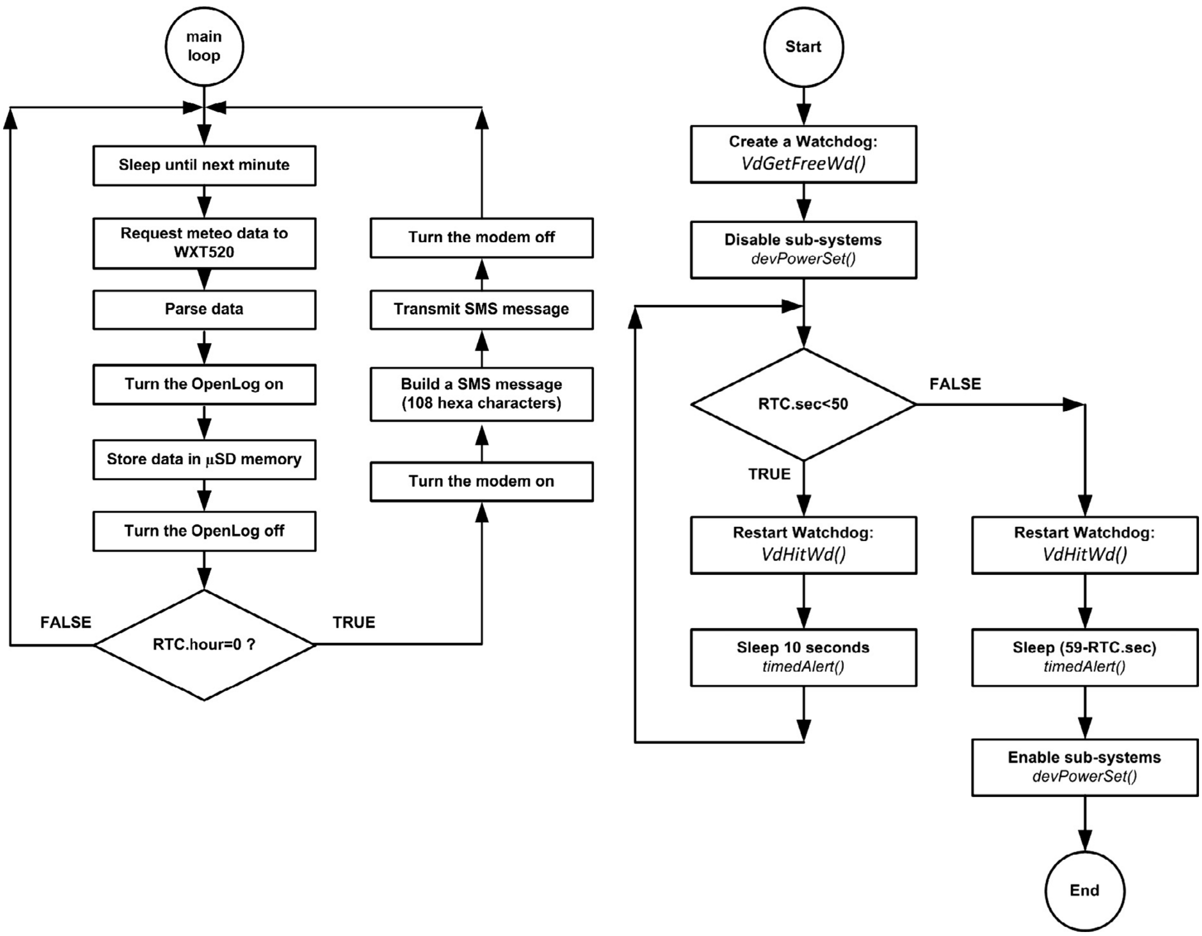


**Fig. 6.** Software flowcharts, (Left) main loop in the embedded controller and (Right) Implementation of sleep cycle using the watchdog service.

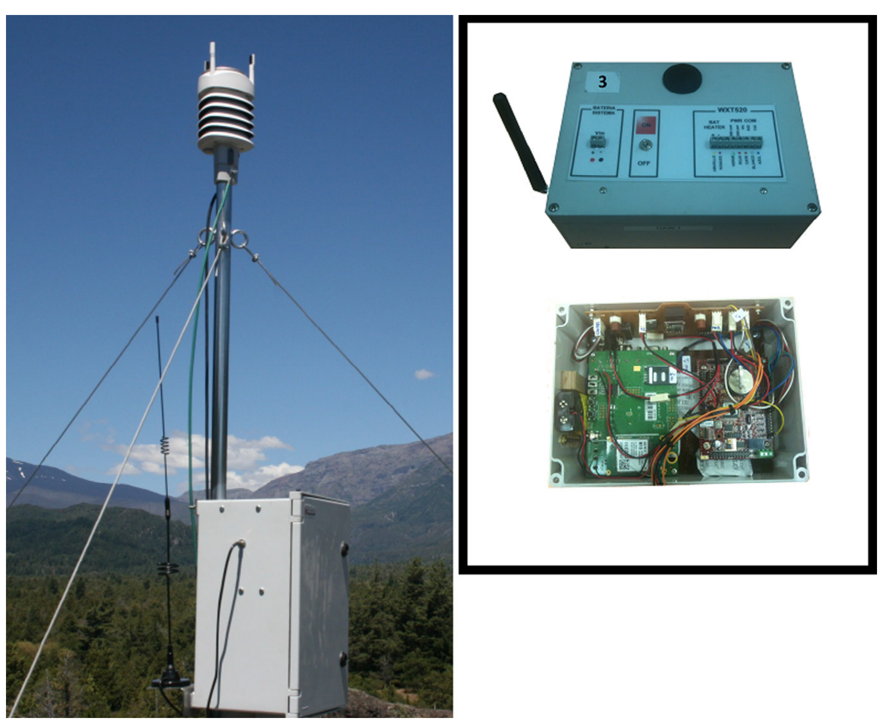

**Fig. 7.** (Left) Endesa meteorological station (St3) and (right) the actual aspect of the custom-made data logger built on the LP3500 embedded controller.

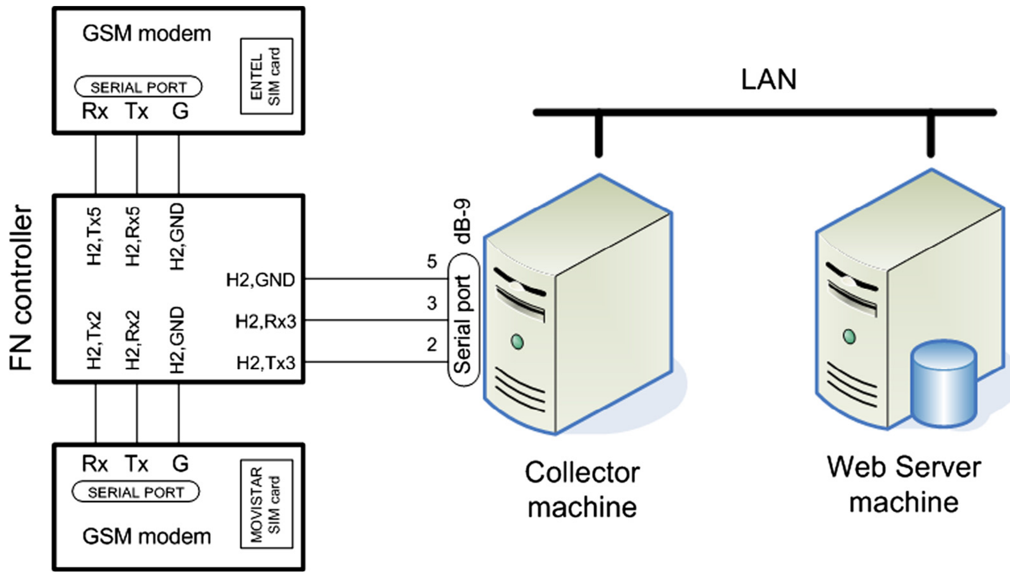


**Fig. 8.** Electrical diagram of base station.

connected to the local area network, it can access to the text file, from which it extracts data to update the PostgreSQL database.

## 3. Experimental results

### 3.1. System performance

In this section we review different aspects associated with the operation of the system, including its characteristics under real conditions, the determination of weaknesses in the original design and the modifications needed to make the system more robust. After building the first prototype enabled with low power features, an AWS was connected in the laboratory using a 12 V & 1.1 A test battery. The AWS transmitted data to the base station for a total of 10 days, resulting in an average current consumption of 4.6 mA. This prototype was programmed using the power-save mode. Considering that the average current used by the multi-sensor is around 2.2 mA, about 50% of energy use is accounted for by the sensors and 50% by the data logger.

A test under field conditions was conducted in November 2013, in which two adjacent stations were set up in Hualqui, a rural area with cellular coverage 50 km from the University of Concepción. The AWSs transmitted over 90% of SMS messages to the base station for a period of 10 days. SMS messages were decoded to obtain meteorological data and all received data were consistent with the data stored on the stations. After this satisfactory test, the watchdog service was not included in the prototype.

After all units were assembled, the seven St1-St7 AWSs were set up in the Laja Valley in February 2014, as detailed in Tables 1 and 6. For the first two months of operation at field, only St5 and St6 stations transmitted data without interruption, while the other stations only functioned for a few days: St1 for 6.6 days, St2 for 10 days, St3 for 9.8 days, St4 for 10.2 days and St7 for 13.6 days. A maintenance visit in April 2014 was carried out to determine why stations St1, St2, St3, St4 and St7 had stopped their operation. A hardware failure on the power unit was found only in station St4. As it will be explained in next paragraphs, the remaining stations stopped due to electromagnetic effects during *Puelche* winds, particularly intense at the highest stations.

In order to prevent further shutdowns of the AWS, the firmware was redesigned to incorporate the use of the watchdog service. Thus, the use of the power-save mode in the original firmware was combined with the watchdog to allow the AWS to recover from a fault condition. Once all the stations were updated with the watchdog service in August 2014, its effect was mostly observed at station St7, which in several occasions was restarted by the watchdog, thus avoiding long data interruptions. Indeed, on certain exceptional days the station restarted more than ten times. Station St7 is located at an electrical generation plant a few meters from high-voltage electrical towers. Because the data logger is mounted on a plastic cabinet, it may be exposed to intense electromagnetic fields that alter its normal operation, in particular when it is reinitiated from power-save mode. Stations St1 and St3 sent start messages four times in seven months. Station St2 did not send start messages as it has no GSM modem. Stations St4, St5 and St6 never sent start messages, because they are located far enough from the intense effect of *Puelche* winds (stronger at east Stations).

The response of station St7 after updating it with the watchdog service suggests that the interruptions occurred in February 2014 were triggered by an external effect that disabled the processor from exiting the power-save mode. Similar to what was observed in station St7, which was subject to excessive electromagnetic activity from the electrical plant, stations St1–St3 appear to have failed due to the electromagnetic effect of environmental conditions during *Puelche* winds (see Fig. 11). This concurs with local observations of intense static electricity during *Puelche* events associated with their very low humidity and high wind conditions.

An eighth station called St8, installed during the maintenance visit in August 2014, was located between St3 and St4 stations. Considering that this station was located in a secure private place, we opted for a power unit supported by a solar panel. The firmware in this case made use of the power-save mode unnecessary while maintaining the use of the watchdog service. From August 9, 2014, to February 24, 2015, stations St2 to St8 transmitted data to the base station without interruption. Station St1 restarted operations in October 2014 because climatic conditions prevented doing it along with the other stations in August 2014.

During the maintenance visit in March 2015 we discovered that stations St1 and St2 had stopped operating on February 24, 2015, despite the operation under of the watchdog service. Notably, the two stations stopped working at almost the same time, St1 station 10 min before St2 station. A few hours later a *Puelche* event of large

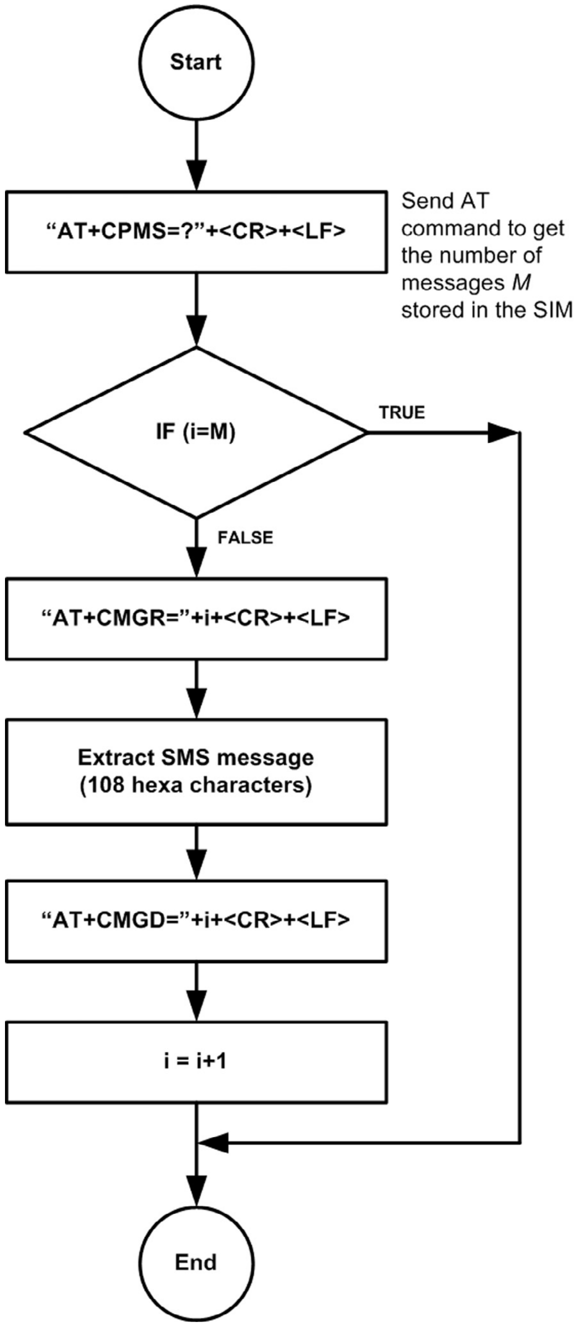


**Fig. 9.** Software flowcharts to get SMS messages arriving to the base station.

intensity was registered at station St3, as can be noted in the right-hand panels of Fig. 11. Although the watchdog service had worked several times in the period August 2014–February 2015, this time the electromagnetic activity of the *Puelche* event was strong enough to not only disable the power-save mode but also the watchdog service. In the following months, stations St1, St2 and St7 were upgraded to be powered by solar panels and thus the power-save mode was disabled, while maintaining the watchdog active. Station St7 no longer required excessive restarts, while stations St1 and St2 operated without interruptions, although a few months later the solar panel was stolen from St1.

During the following maintenance visit to the stations, it was found that the data stored in the micro SD memory of station St6 was corrupted and it was not possible to read the data. Although the station had been transmitting data correctly, at some point after the previous visit in October 2014, the Openlog or the micro SD card failed. The Openlog along with the SD card of station St6 operated correctly for at least 9 months after it was put into operation in the field in February 2014. In subsequent maintenance visits, including the last one in January 2016, other micro SD cards in the field showed the same failure as that of the micro SD card at station St6. Working on the assumption that malfunction was caused by moisture, all the Openlogs and micro SD cards were replaced by new units during the last visit. It has not been possible to reproduce the error under laboratory conditions nor has the supplier been able to detect the problem, but probably only the micro SD cards failed, since the replaced Openlogs worked fine when they were tested separately with new SD cards.

As in the initial tests performed at Hualqui, the GSM cellular transmission system has proven to be robust. Fig. 12 shows a high rate of SMS messages received in a period of four months. For 78% of the days in this period the six stations, St3–St8, transmitted 144 messages per day (6 multiplied by 24), that is all of the messages that should have been sent every day (station St2 did not have cellular coverage and station St1 had intermittent cellular coverage).

### *3.2. Meteorological analysis*

Fig. 11 illustrates the occurrence of two *Puelche* events detected by the EMN network. The three lower graphs in the left-hand column of Fig. 11, describe in detail the *Puelche* event measured at station St3. The third and fourth graphs show the wind direction (Dm) and the speed maximum (Sx), respectively. From February 13, 2014, the wind is mainly from the east (Dm is around 90°) for around 1.5 days, and its magnitude is above the magnitude of daily wind cycle. The wind speed on station St3 reaches a maximum of 20.5 m/s in this period. As it is shown in the second graph, the *Puelche* wind is associated with an abrupt temperature increase, while humidity levels fall significantly to 18.2%. The *Puelche* event was detected by the first five stations (St1–St5), while it was almost imperceptible at St6 and totally imperceptible at St7, as it can be seen on the first graph. Similarly, the three lower graphs in the right-hand column of Fig. 11, describe the *Puelche* event on February 25, 2015.

Fig. 13 shows a register at one-minute intervals of zonal winds and temperature at three stations in the network. The arrival of a wind pulse from the east can be observed clearly (maximum acceleration), accompanied at the same time by abrupt warming. Temperature jumps range from about 0.1 °C/min at St1 to more than 0.6 °C/min at St2. A simple calculation of the propagation speed (vertical component) of the warm wind pulse that descends the Laja River Valley gives a value of 4.6 m/min (0.08 m/s) in every section (right hand panel in Fig. 13).

Fig. 14 illustrates other results obtained from the deployment of the EMN along the Laja River Valley. In this case, we took advantage of the availability of high-resolution measurements of atmospheric pressure and surface wind at several points along the valley to make a preliminary analysis of the relationship between the surface pressure field and the occurrence of events of intensified easterly winds. Fig. 14a shows the evolution of air pressure averaged over stations St2, St3, St4, St5, and St7 for the period from August 9 to October 31, 2014, encompassing the last part of the austral winter and the beginning of spring. Synoptic perturbations produced marked inter-daily variability in the pressure field, especially in the first half of the period when deviations from the mean reached up to ±10 hPa. Fig. 14b shows the pressure differences among the stations and the average among them. A clear grouping of the stations is noted in this Figure, with pressure in the eastern part of the valley (stations St2, St3, colors blue and black) varying in opposite phase to that of the western stations (stations St4, St5, St7, represented in green, magenta, and red, respectively). Phase

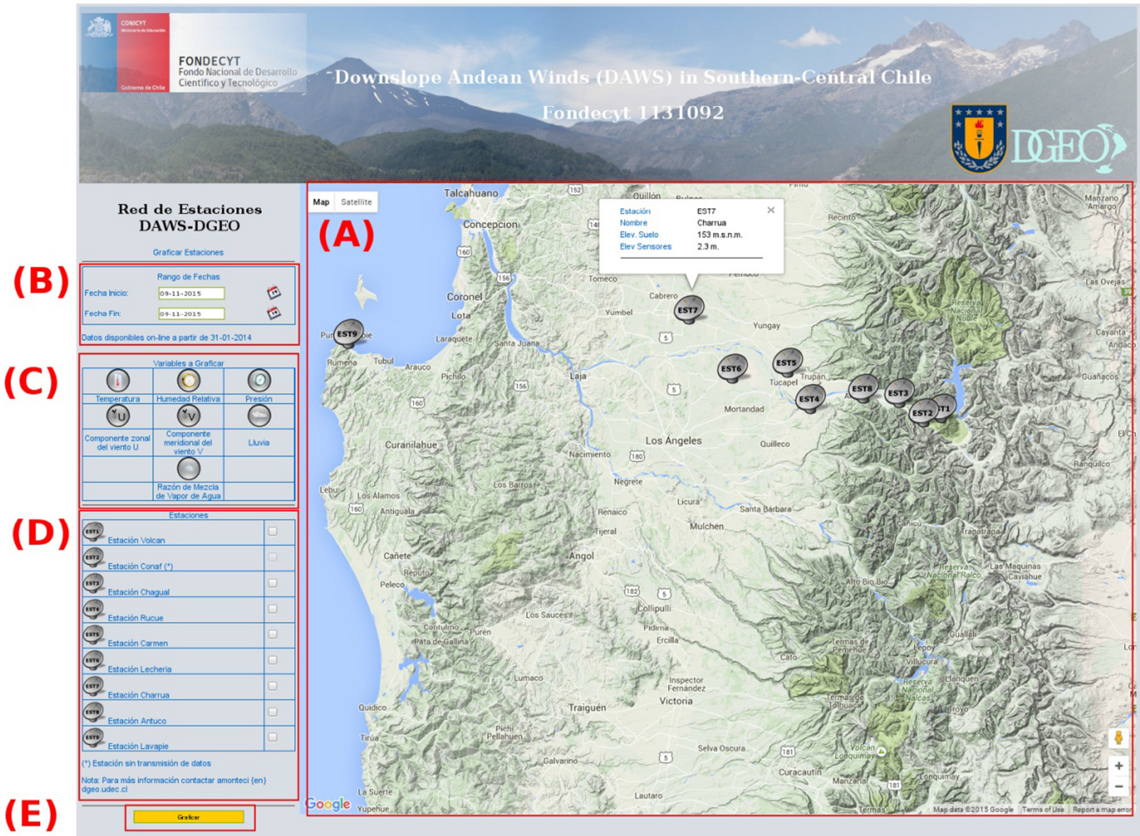


**Fig. 10.** Web interface to access data from the meteorological stations. (A) map of the study area, (B) selection of period of time, (C) selection of variables, (D) selection of stations, (E) update button.

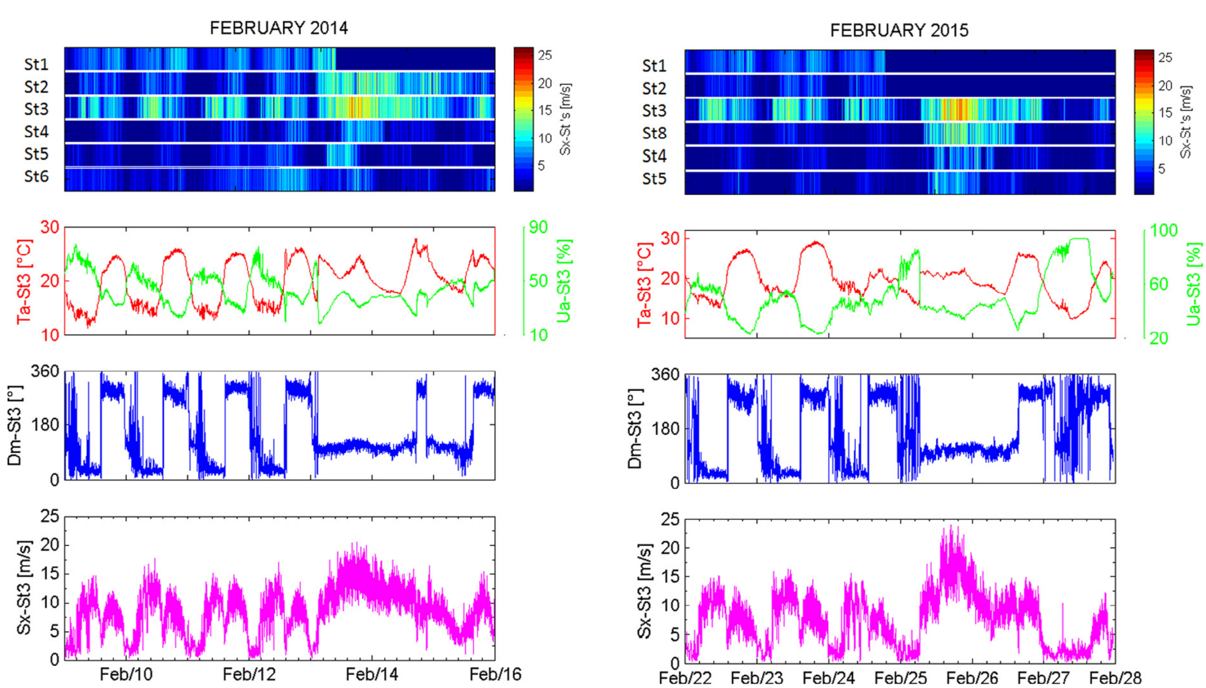


**Fig. 11.** *Puelche* events detected by the network of stations. The six lower graphs compare two events measured at station St3. The event in February 2015 (right column) involved winds of up to 24 m/s, while in February 2014 (left column) winds reached velocities of 20.5 m/s.

opposition can produce significant zonal pressure gradients of up to 4 hPa in about 60 km and thus drive the zonal component of winds along the valley. Indeed, Fig. 14c shows the surface easterly wind averaged among stations St2, St3, and St8. Periods of enhanced easterly winds generally correspond to *Puelche* events, which in the first half of the period were more frequent and intense

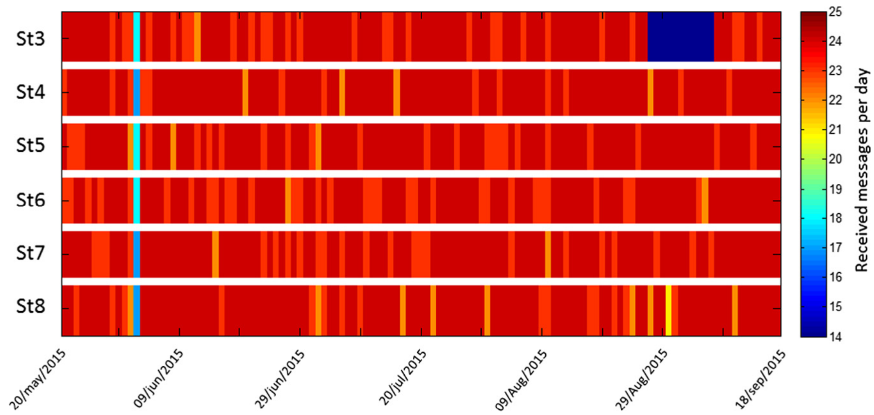


**Fig. 12.** Rate of SMS messages received by the server from 6 stations. Every station sent 24 messages per day via a GSM cellular modem. In the period covered in the figure, the server received all the messages sent on 78% of the days.

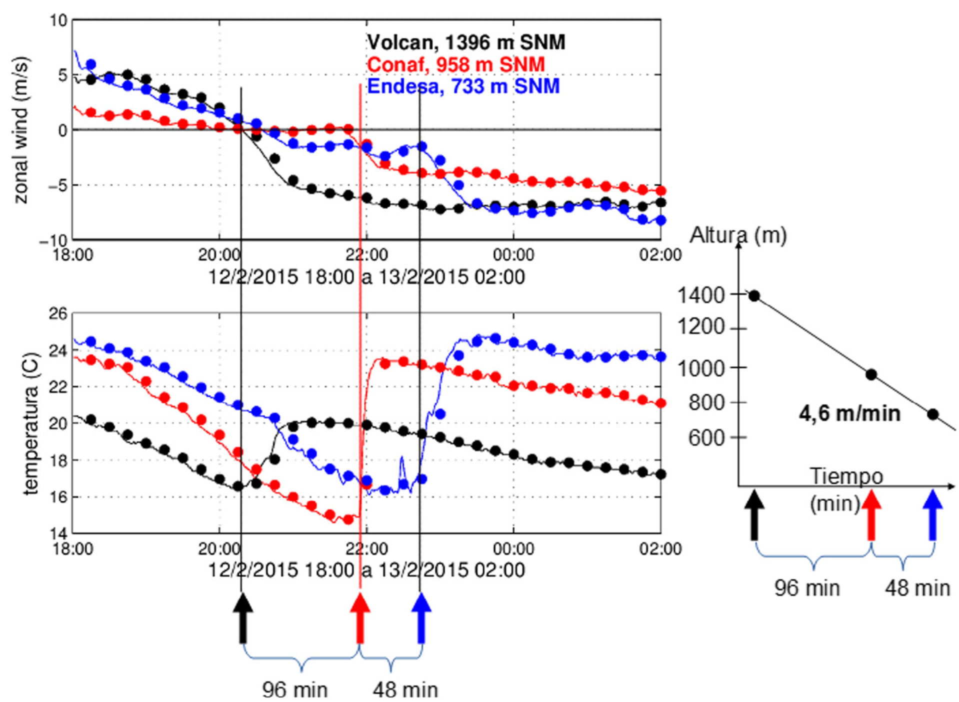


**Fig. 13.** Time series of the zonal wind component (upper panel, m/s) and temperature (lower panel, °C) close to the surface, registered at stations Volcán, St1 (black line), Conaf St2 (red line) and Endesa St3 (blue line) in one minute intervals. The circles indicate averages for every fifteen minutes. The right panel shows an altitude/time reading of the beginning of the *Puelche* wind pulse. (For interpretation of the references to color in this figure legend, the reader is referred to the web version of this article.)

(anomalies above 5 m/s). A general association between the zonal pressure gradient (Fig. 14b) and the occurrence of *Puelche* events (Fig. 14c) can be observed, although it was less marked in the spring. Future work will analyze in more detail the full dataset produced by the monitoring network in order to more quantitatively establish the relationship between the pressure field and *Puelche* winds and improve the understanding of their dynamical forcing.

## 4. Conclusions

Data generated by the EMN system allowed for a high resolution characterization of downslope winds locally known as *Puelche* winds. At present, a climatological analysis of their occurrence and the associated impacts has been performed based on gridded reanalyzed data, after a comparison with observations from the EMN system [2]. Also, the analysis of the dynamics controlling the presence of *Puelche* winds far from the valley mouth, based on observations in the Laja river valley along with numerical simulations, is the subject of a future manuscript.

According to the characteristics of the study area, the design and construction of the network of weather stations was conceived especially for low energy consumption. This work presented guidelines to develop a power-efficient monitoring system based on an embedded controller. Energy efficient systems are especially necessary to operate in low temperature environments and/or where it is not possible to use large energy generating sources. Stations are a hybrid between a commercial meteorological multi-sensor and an embedded controller. The multi-sensor provided a power-efficient operation, while the embedded controller allowed designing in an integrated and flexible platform. The whole system is flexible as most parts have been customized and, thus, it can be

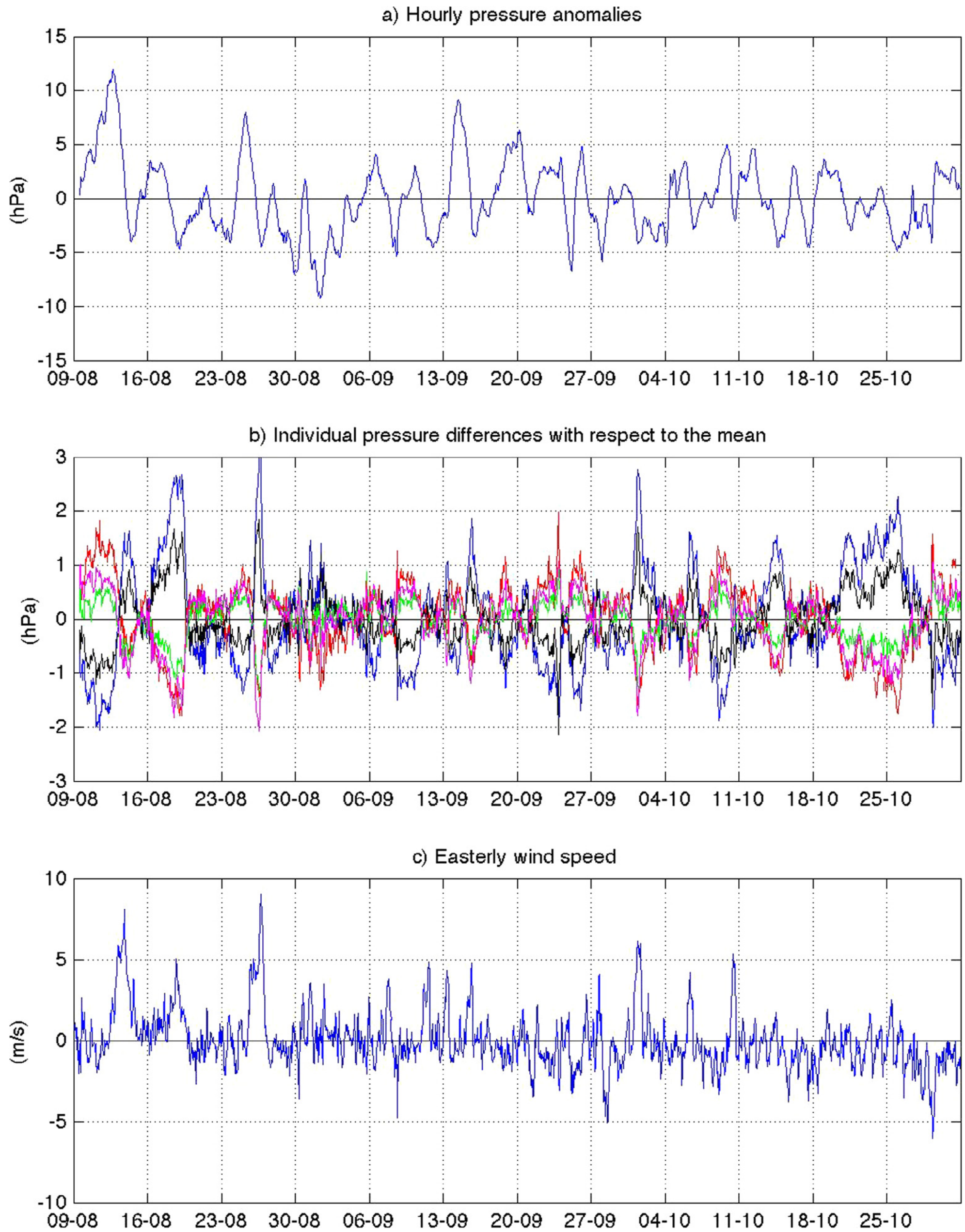


**Fig. 14.** Relationship between pressure field and easterly surface winds in Laja Valley between August 9 and October 31, 2014. (a) Pressure anomalies (with respect to the mean in the period) averaged for stations St2, St3, St4, St5, and St7. (b) Difference between each station's pressure and the mean in (a). Color codes: station St2-blue, station St3-black, station St4-green, station St5-magenta, station St7-red. (c) Easterly wind component averaged among stations St2, St3, and St8. In all panels, hourly averages of the basic data are used and the mean diurnal cycles of each series has been removed. (For interpretation of the references to color in this figure legend, the reader is referred to the web version of this article.)

easily maintained, expanded and updated. Practical problems were identified and helped to improve the original design. First, the static electricity associated with intense *Puelche* events and electromagnetic interference from nearby sources affected the operation of three of the eight stations, pointing to the need of mounting the stations on properly grounded metal cabinets. Second, after months of continuous operation some failures on the micro SD memory cards suggest the need to replace and test new memory cards and micro SD card drivers.

The EMN system stores data at a rate of one record per minute. This high-frequency data is only available after recovery of the micro SD card. The system also provides a near real-time data communication using GSM-SMS technology. To reduce transmission costs, measurements at a rate of 15 min are received in the base station. Data are encoded in SMS messages, which are also used to inform when the system has initiated or when there is a failure condition. Due to the importance of having real-time data, stations located in sites without or with poor cellular coverage will be updated in future projects, using RF modems to transmit the data to a station with good cellular coverage.

## Acknowledgements

This work was supported by the Comisión Nacional de Investigación Científica y Tecnológica (CONICYT) – Chile through Fondecyt grant number 1131092.

## References


[1] D. Linden, T.B. Reddy, Handbook of Batteries, third ed., McGraw-Hill, 2001.

[2] A. Montecinos, R. Muñoz, S. Oviedo, A. Martínez, V. Villagrán, Climatological characterization of Puelche winds down the western slope of the extratropical Andes Mountains using the NCEP climate forecast system reanalysis, J. Appl. Meteorol. Climatol. (2016).

[3] W. Lu, S. Zhong, J.J. Charney, X. Bian, S. Liu, WRF simulation over complex terrain during a southern California wildfire event, J. Geophys. Res. Atmos. 117 (2012) D05125.

[4] A.K. Kochanski, M.A. Jenkins, S.K. Krueger, J. Mandel, J.D. Beezley, Real time simulation of 2007 Santa Ana fires, For. Ecol. Manage. 294 (2013) 136–149.

[5] Y. Fovell, Y. Cao, R.G. Fovell, Downslope windstorms of San Diego County. Part I: A case study, Mon. Weather Rev. 144 (2) (2016) 529–552.

[6] D.M. Amatya, C.A. Harrison, C.C. Trettin, Comparison of potential evapotranspiration (PET) using three methods for a grass reference and a natural forest in coastal plain of South Carolina, in: Proceedings of the 2014 South Carolina Water Resources Conference, 2014.

[7] C. Yonghua, Integration of Sentry™ visibility sensor into Campbell scientific data logger CR1000, Procedia Environ. Sci. 12 (2012) 1137–1143.

[8] F.L. Ogden, W. Lai, R.C. Steinke, J. Zhu, Validation of finite water-content vadose zone dynamics method using column experiments with a moving water table and applied surface flux, Water Resour. Res. 51 (5) (2015) 3108–3125.

[9] J.G. Wilson, A.A. Simpson, K.L. Cummins, J.J. Kiriazes, R.G. Brown, C.T. Mata, Oceanic storm characteristics off the Kennedy space center coast, in: 5th International Lightning Meteorology Conference, Arizona USA, 2014.

[10] E. Ryder et al., Temperature quenching of CDOM fluorescence sensors: temporal and spatial variability in the temperature response and a recommended temperature correction equation, Limnol. Oceanogr. Methods 10 (12) (2012) 1004–1010.

[11] P. Ramamurthy, T. Sun, K. Rule, E. Bou-Zeid, The joint influence of albedo and insulation on roof performance: an observational study, Energy Build. 93 (2015) 249–258.

[12] J. Ardö, H. Abdalla, M. Elkhidir, A. Khatir, F. Cropley, Meteorological measurements in Demokeya, North Kordofan: a contribution to climate change research, Sudan Acad. Sci. J. – Special Issue (Climate Change) 11 (2015) 118–127.

[13] A.B. White et al., A twenty-first-century California observing network for monitoring extreme weather events, J. Atmos. Ocean. Technol. 30 (8) (2013) 1585–1603.

[14] R. Mukaro, A microcontroller-based data acquisition system for solar radiation and environmental monitoring, IEEE Trans. Instrum. Meas. 48 (6) (1999) 1232–1238.

[15] M. Benghanem, Measurement of meteorological data based on wireless data acquisition system monitoring, Appl. Energy 86 (12) (2009) 2651–2660.

[16] F. Shariff, N.A. Rahim, W.P. Hew, Zigbee-based data acquisition system for online monitoring of grid-connected photovoltaic system, Expert Syst. Appl. 42 (3) (2015) 1730–1742.

[17] P.A. Kulkarni, V.V. Yerigeri, An economical weather monitoring system based on GSM using solar and wind energy, Int. J. Adv. Technol. Innov. Res. 7 (2015) 0263–0268.

[18] M. Srbinovska, C. Gavrovski, V. Dimcev, A. Krkoleva, V. Borozan, Environmental parameters monitoring in precision agriculture using wireless sensor networks, J. Clean. Prod. 88 (2015) 297–307.

[19] K. Lokesh, K. Associate, J. Madhuri, K. Anuradha, A Zigbee based energy efficient environmental monitoring alerting and controlling system, in: International Conference on Information Communication and Embedded Systems (ICICES), 2016, pp. 1–7.

[20] A.R. Al-Ali, I. Zualkernan, F. Aloul, A mobile GPRS-sensors array for air pollution monitoring, IEEE Sens. J. 10 (10) (2010) 1666–1671.

[21] S. Rosiek, F.J. Batlles, A microcontroller-based data-acquisition system for meteorological station monitoring, Energy Convers. Manage. 49 (12) (2008) 3746–3754.

[22] D.K. Fisher, H. Kebede, A low-cost microcontroller-based system to monitor crop temperature and water status, Comput. Electron. Agric. 74 (1) (2010) 168–173.

[23] J.-A. Jiang et al., A GSM-based remote wireless automatic monitoring system for field information: A case study for ecological monitoring of the oriental fruit fly, Bactrocera dorsalis (Hendel), Comput. Electron. Agric. 62 (2) (2008) 243–259.

[24] J.T. Devaraju, K.R. Suhas, H.K. Mohana, V.A. Patil, Wireless portable microcontroller based weather monitoring station, Measurement 76 (2015) 189–200.

[25] K. Hyder, B. Perrin, Embedded Systems Design using the Rabbit 3000 Microprocessor, Elsevier, 2005.

[26] C.-Y. Liu et al., Development of an embedded system-based gateway for environmental monitoring using wireless sensor network technology, in: Fifth International Conference on Sensing Technology (ICST), 2011, pp. 544–548.

[27] H.F. Rezaei, N. Sitter, A. Kruger, Next generation system for real-time monitoring of rainfall, soil moisture, and soil temperature, in: SAS 2011 – IEEE Sensors Applications Symposium, Proceedings, 2011, pp. 70–75.

[28] M. Gagliarducci, D.A. Lampasi, L. Podesta, GSM-based monitoring and control of photovoltaic power generation, Measurement 40 (3) (2007) 314–321.

[29] I.A. Aziz, H. Hasan, J. Ismail, M. Mehat, Remote monitoring in agricultural greenhouse using wireless sensor and short message service (SMS), Int. J. Eng. Technol. IJET 9 (9) (2009) 1–12.

[30] C.-L. Tseng et al., Feasibility study on application of GSM – SMS technology to field data acquisition, Comput. Electron. Agric. 53 (2006) 45–59.

[31] A. Amin, M.N.A. Khan, A survey of GSM technology to control remote devices, Int. J. Sci. Technol. 7 (6) (2014) 153–162.

[32] V. Oyj, User's Guide, Vaisala Weather Transmitter, WXT520, Helsinki, Finland, 2010.

[33] C.K. Yu et al., Measuring droplet fall speed with a high-speed camera: Indoor accuracy and potential outdoor applications, Atmos. Meas. Tech. 9 (4) (2016) 1755–1766.

[34] B.W. Butler et al., High-resolution observations of the near-surface wind field over an isolated mountain and in a steep river canyon, Atmos. Chem. Phys. 15 (2015) 3785–3801.

[35] L. Tao, K. Sun, D.J. Miller, D. Pan, L.M. Golston, M.A. Zondlo, Low-power, open-path mobile sensing platform for high-resolution measurements of greenhouse gases and air pollutants, Appl. Phys. B Lasers Opt. 119 (1) (2015) 153–164.

[36] A. Salmi, J. Ikonen, Piezoelectric precipitation sensor from Vaisala, in: WMO Technical Conference on Instruments and Methods of Observation (TECO-2005), Bucharest, Romania, 2005, pp. 4–7.

[37] Fox (LP3500) C-Programmable Single-Board Computer User's Manual, California USA.